CHAPTER 3 – DEFECT DEFINITION

In Chapter 2, velocity images obtained from three-dimensional tomographic reconstruction method (CSLT) were discussed. The principal use of CSLT is the identification of low-velocity regions indicative of anomalies in a drilled shaft. However, the velocity distributions or histograms are often smoothly varying so that identification of a single cutoff velocity, below which the shaft is considered to be defective, is difficult. In this chapter, a statistically definition of a "defect" in a drilled shaft foundation is presented. By fitting classical normal probability distributions to the velocity histogram, the probability that any element (velocity bin) in the model volume is defective is quantified. In this approach, the probability of the total defective volume exceeding some threshold can be defined, and therefore engineers can make risk-based assessments of shaft integrity.

In the next section, a robust curve-fitting technique is presented to decompose histograms of crosshole sonic logging (CSL) velocity tomograms into one, two, or three constituent normal distributions (Gaussians). The crossover between the Gaussian with the lowest mean velocity and its nearest neighbor provides a practical definition of cutoff velocity for low-velocity flaw definition. Although the approach is limited in the test data by the presence of artifacts from the tomographic inversion, velocities below 85-90% of the median shaft velocity appear to be indicative of flaws.

3.1 STATISTICAL MODELING - GAUSSIAN PROBABILITY DISTRIBUTION CURVES

The statistical Gaussian curve-fitting technique is used for the final 3-D velocity distribution produced by tomographic inversion, following all data editing, velocity equalization corrections, and processing. The velocity histogram is the primary data; results are relatively insensitive to velocity bin widths <50 m/s. Therefore, in these examples, an optimum velocity bin size of 25 m/s is used. A robust (L1-norm) curve-fitting procedure is used to decompose the observed histogram into 1, 2, or 3 normal distributions (Gaussians). The mean (μ), standard deviation (σ), and amplitude (A) of each Gaussian component are the fitted parameters. An F-test is used to determine the probability that the additional Gaussian have actually improved the fit. PF_{12} is, therefore, the probability that the 2-Gaussian fit is better than the 1-Gaussian fit; similarly PF_{23} is the probability that 3 Gaussians is superior to 2. The quantity PF_{13} is also reported for completeness. PF values near 50% indicate there is no significant improvement using additional Gaussian, whereas PF = 100% means that the more complex fitting is unquestionably more accurate.

One of the Gaussians is identified as being associated with the anomalies of interest. For the 2-Gaussian case this is obviously the distribution with the smaller mean velocity, but for the 3-Gaussian fits either of the smaller-mean distributions could be relevant. For the data analyzed here, however, the Gaussian with the lowest mean velocity is inferred as anomalous concrete.

3.2 STATISTICAL MODELING RESULTS

The best fits for one-, two-, and three-Gaussian applied to two shafts at the Amherst test site are summarized in Table 1. Note that for each shaft, some trial-and-error adjustment of the starting parameter values was necessary in order to obtain reasonable results. In other words, the procedure is not yet completely automated and some analyst skill is required.

Multi-offset CSL data for Amherst Shaft 1 was tomographically inverted using low and high smoothing values of 0.1 and 1.0, respectively. The smoothing parameter controls the trade-off between data goodness-of-fit and model smoothness. The best fit may lead to a model with unrealistic (rough) velocity variations, whereas an over smoothed model may not have an acceptable model fit. The statistical fits reflect the differences in model smoothness.

Analysis of the low-smoothing solution for Shaft 1 is shown in Figure 18. A single Gaussian is a reasonable approximation to the velocity distribution as a whole. A second Gaussian fits a visually obvious low-velocity extension to the main distribution, but the F-test does not indicate this is statistically significant. Adding the third Gaussian does result in a significant improvement according to the F-test. The transition from the anomalous low-velocity portion occurs at 3,625 m/s (12,000 ft/s), which is 90% of both the mean and median velocity. The 3-D distributions of portions of the shaft indicated by the tomography to lie below this cutoff, and hence be part of a flaw, are also depicted in Figure 18.

High smoothing (Figure 19) during the tomographic inversions produces a smoother model as expected, but a pronounced hump in the histogram is now apparent at intermediate velocity (~3,900 m/s, 12,800 ft/s). Although a very low-velocity tail is again visually obvious, statistically only the 2nd Gaussian is important in making up the large misfits to a single Gaussian introduced by the intermediate-velocity hump. Selecting the high side of this feature as the flaw cutoff results in a cutoff velocity fully 95% of the mean or median velocities and therefore too much of the shaft is interpreted as flawed. Selecting the low side transition to the low-velocity tail yields a cutoff velocity of 91% of the mean or median, now in better agreement with the low-smoothing result for the same shaft. The intermediate-velocity feature is interpreted as a tomographic artifact, but its origin is unknown. These velocities are distributed around the regions of the inferred flaws and are not simply streaked along one side, as would be the case if one panel had not been properly static corrected. The artifact appears to be intrinsic to the Tomographic inversion procedure.

For Amherst Shaft 4, the intermediate-velocity artifact is now very pronounced, having the highest amplitude of any of the sub-distributions (Figure 20). However, this is now for a low-smoothing tomographic solution, not high smoothing as previously. (In view of that, the high smoothing results is not presented). Now the cause of the artifact can be likely identified as incomplete or ineffective static corrections, because the intermediate-velocity anomalies are vertically streaked throughout the shaft. Again, this intermediate-velocity distribution allows two locations to be picked for a velocity cutoff: the high-side value of 96% of the median or mean is clearly incorrect; the low-side value of 89% of the median or 90% of the mean is in better agreement with previous results. In both of these last two cases, the inferred upper cutoff may have been influenced by the artifacts.

The Gaussian fitting statistical analysis result presented in this section on Amherst Shafts 1 and 4 are developed for demonstrating the basic concept. In Section 5.2, the Amherst tomography results are presented based on multi-zone statistical analysis of the data with more refined definition of defects at each separate defect zone.

Table 1. Normal-Distribution Fitting to Amherst CSL Tomography (CSLT).

	Shaft 1 Low Smoothing	Shaft 1 High Smoothing	Shaft 4 Low Smoothing
μ_{11} (m/s)	4,050	4,130	3,760
σ_{11} (m/s)	210	110	270
A_{11} (counts/bin)	4,900	8,400	5,450
μ_{12} (m/s)	4,050	4,140	3,830
σ_{12} (m/s)	210	100	230
A_{12} (counts/bin)	4,910	8,800	3,600
μ_{22} (m/s)	3,290	3,880	3,590
σ_{22} (m/s)	150	80	50
A_{22} (counts/bin)	190	2,100	3,400
PF_{12}	66%	100%	100%
V_{cutoff} (m/s)	3,450	3,950	3,625
V_{cutoff}/μ_{11}	85%	96%	96%
V_{cutoff}/V_{median}	85%	96%	96%
μ_{13} (m/s)	4,210	4,140	3,800
σ_{13} (m/s)	150	100	230
A_{13} (counts/bin)	4,000	8,800	3,560
μ_{23} (m/s)	3,520	3,890	3,590
σ_{23} (m/s)	290	60	50
A_{23} (counts/bin)	250	2,100	3,750
μ_{33} (m/s)	3,900	3,630	3,150
σ_{33} (m/s)	120	200	70
A_{33} (counts/bin)	3,200	260	90
PF_{23}	100%	69%	35%
PF_{13}	100%	100%	100%
V_{cutoff} (m/s)	3,625	3,925 (3,750)	3,625 (3,375)
V_{cutoff}/μ_{11}	90%	95% (91%)	(90%)
V_{cutoff}/V_{median}	90%	95% (91%)	(89%)

* μ_{12} : mean velocity of the first Gaussian in a 2-Gaussian fit
σ_{23} : standard deviation of the second Gaussian in a 3-Gaussian fit
A_{33}: amplitude of the third Gaussian in a 3-Gaussian fit
PF_{23}: the probability that 3 Gaussians is superior to 2
V_{cutoff}: cut-off velocity
V_{median}: median velocity

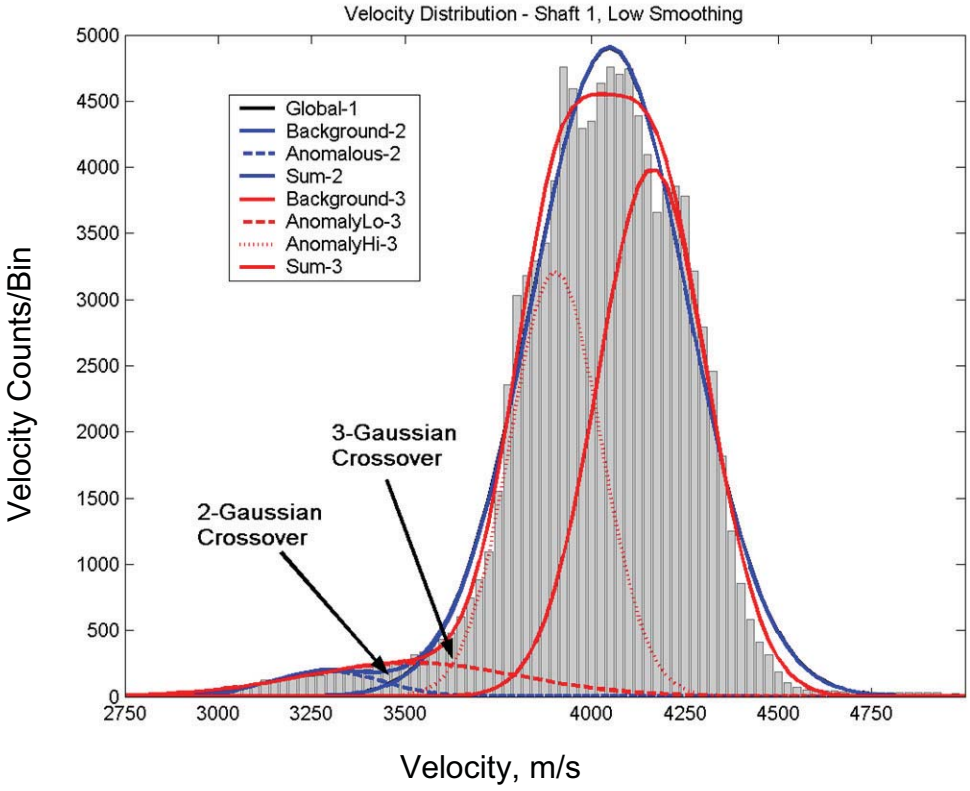
Velocity Distribution - Shaft 1, Low Smoothing
Global-1
Background-2
Anomalous-2
Sum-2
Background-3
AnomalyLo-3
AnomalyHi-3
Sum-3
3-Gaussian Crossover
2-Gaussian Crossover
Velocity Counts/Bin
Velocity, m/s
5000
4500
4000
3500
3000
2500
2000
1500
1000
500
0
2750
3000
3250
3500
4000
4250
4500
4750

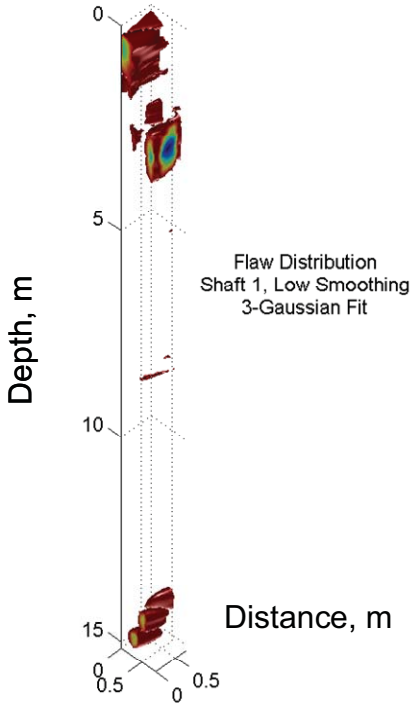

Figure 18. Schematic. Top. Histogram of Velocities from 3-D Tomography (CSLT) (Shown in Gray) of Amherst Shaft 1 under Low Smoothing, with Multi-Gaussian Fits Superimposed. Bottom. Visualization of Inferred Flawed Portions of the Shaft.

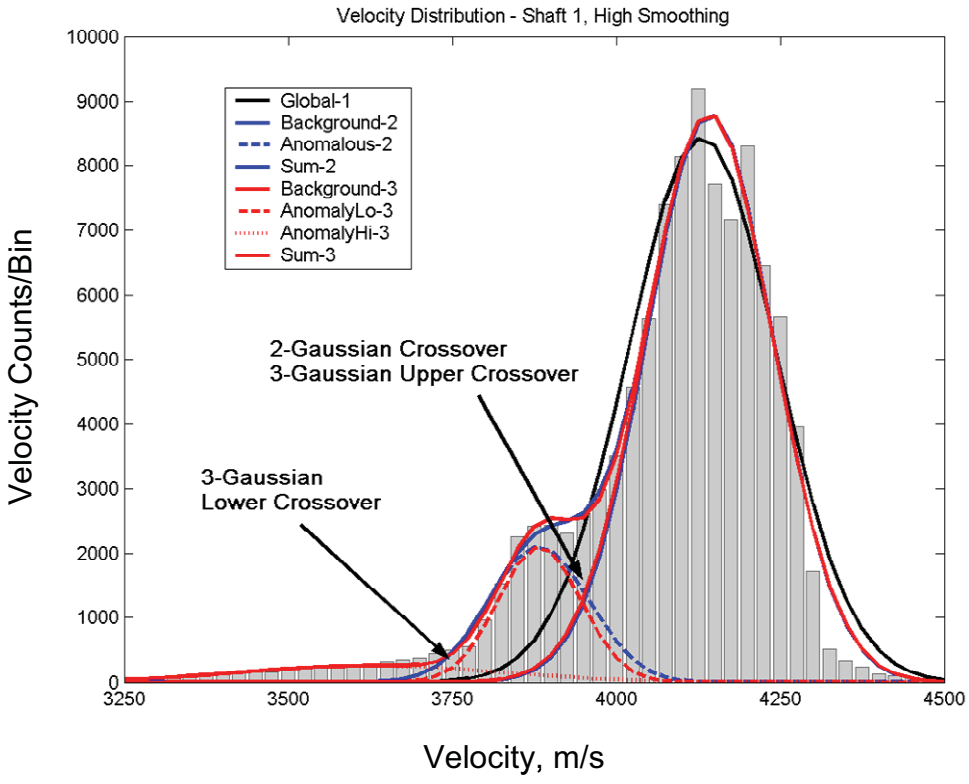

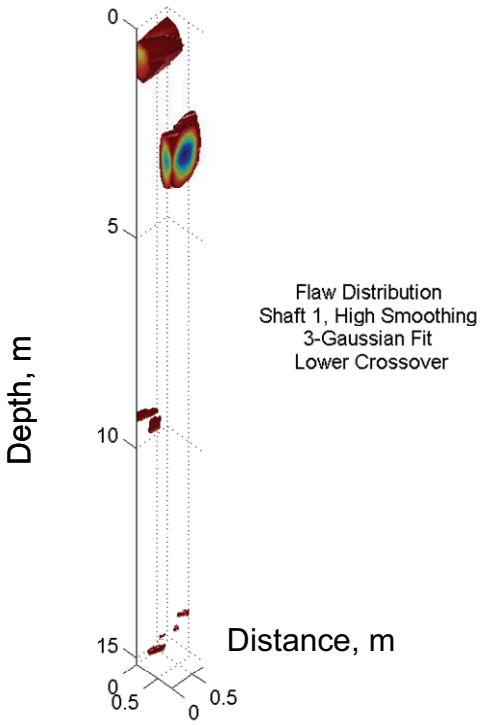

Figure 19. Schematic. As Figure 18 for Amherst Shaft 1, but for High Smoothing. Note Development of Anomalous Zone at Intermediate Velocities.

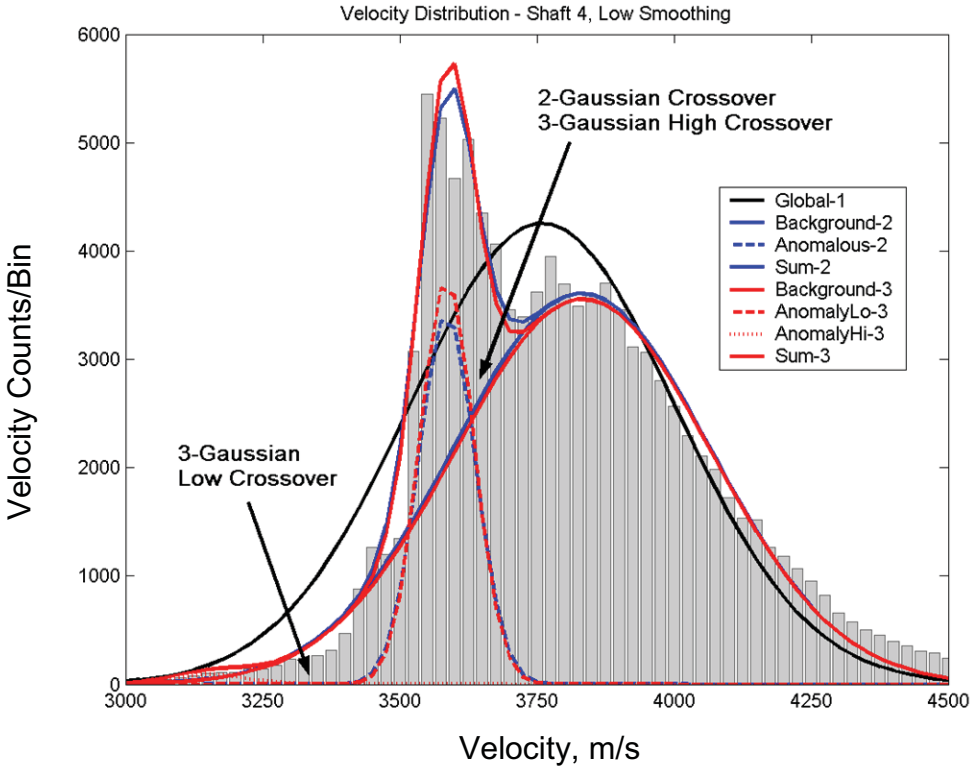

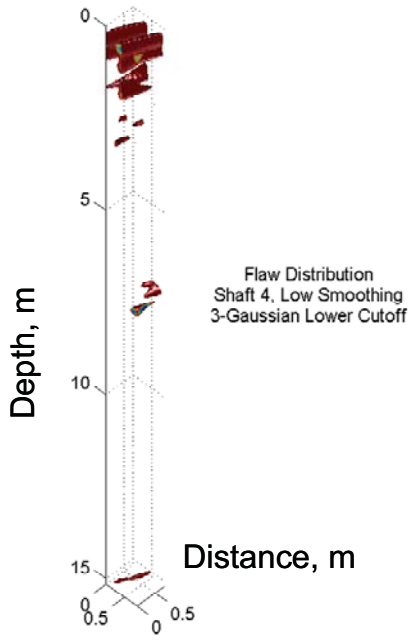

Figure 20. Schematic. Velocity Histogram and Flaw Interpretation for Amherst Shaft 4, Low Smoothing. Note Very Pronounced Intermediate-Velocity Artifact.